

# THE ORIENTATION OF $\beta$ -SHEETS IN PORIN. A POLARIZED FOURIER TRANSFORM INFRARED SPECTROSCOPIC INVESTIGATION

E. NABEDRYK,\* R. M. GARAVITO,<sup>‡</sup> AND J. BRETON\*

\**Service de Biophysique, Département de Biologie, CEN Saclay 91191 Gif-Sur-Yvette Cedex, France*  
and <sup>‡</sup>*Department of Biochemistry and Molecular Biology, University of Chicago, Illinois 60637*

**ABSTRACT** The orientation of the protein secondary structures in porin is investigated by Fourier transform infrared (FTIR) linear dichroism of oriented multilayers of porin reconstituted in lipid vesicles. The FTIR absorbance spectrum shows the amide I band at  $1,631\text{ cm}^{-1}$  and several shoulders around  $1,675\text{ cm}^{-1}$  and at  $1,696\text{ cm}^{-1}$  indicative of antiparallel  $\beta$ -sheets. The amide II is centered around  $1,530\text{ cm}^{-1}$ . The main dichroic signals peak at  $1,738$ ,  $1,698$ ,  $1,660$ ,  $1,634$ , and  $1,531\text{ cm}^{-1}$ . The small magnitude of the  $1,634\text{ cm}^{-1}$  and  $1,531\text{ cm}^{-1}$  positive dichroism bands demonstrates that the transition moments of the amide I and amide II vibrations are on the average tilted at  $47^\circ \pm 3^\circ$  from the membrane normal. This indicates that the plane of the  $\beta$ -sheets is approximately perpendicular to the bilayer. From these IR dichroism results and previously reported diffuse x-ray data which revealed that a substantial number of  $\beta$ -strands are nearly perpendicular to the membrane, a model for the packing of  $\beta$ -strands in porin is proposed which satisfies both IR and x-ray requirements. In this model, the porin monomer consists of at least two  $\beta$ -sheet domains, both with their plane perpendicular to the membrane. One sheet has its strands direction lying nearly parallel to the membrane normal while the other sheet has its strands inclined at a small angle away from the membrane plane.

## INTRODUCTION

Porin (OmpF) is a trimeric integral membrane protein forming transmembrane channels across *E. coli* outer membranes. A 3-D image of the protein, as visualized by electron microscopic and diffraction measurements on 2-D arrays of porin reconstituted in lipid vesicles, (1, 2) clearly shows pores passing through the membrane. Previous infrared (IR) and circular dichroism measurements indicate that the secondary structure of porin consists predominantly of antiparallel  $\beta$ -sheets (3, 4). Furthermore, the x-ray diffraction pattern of 3-D crystals of porin is consistent with a significant number of  $\beta$ -strands oriented approximately perpendicular to the presumed membrane plane (4, 5). The overall orientation of all the  $\beta$ -strands as well as of the  $\beta$ -sheet planes themselves, which would allow a more detailed description of the molecular organization of these secondary structures responsible for the formation of the pore, remains however unknown.

The degree of orientation of the secondary structures in a membrane protein can be investigated by IR dichroism of oriented multilayer films of the native membrane or of liposomes in which this protein has been incorporated. Using this spectroscopic approach, the transmembrane

arrangement of  $\alpha$ -helices has been demonstrated in bacteriorhodopsin (6–9), rhodopsin (10, 11), cytochrome oxidase (12), and several reaction centers and antenna complexes from photosynthetic membranes (7, 13–16).

Here, we report new data on the conformation and on the orientation of the dominant protein secondary structure in porin by analyzing Fourier transform IR (FTIR) linear dichroism spectra of oriented films of porin reconstituted in lipid vesicles. Together with the x-ray data (4, 5), our IR results allow to estimate the average orientation of both the plane of the  $\beta$ -sheet and the  $\beta$ -strand directions with respect to the membrane plane.

## MATERIALS AND METHODS

Porin (1.0 mg/ml) was reconstituted in DMPC vesicles (protein/lipid = 1/1 by weight) as described in 2 for the investigation of 2-D crystals by electron microscopy and image processing. This procedure was analogous to the reconstitution method leading to functional pores (2, 17). Orientation of the membranes was achieved by air-drying the suspension in distilled water onto  $\text{CaF}_2$  discs. FTIR spectra were recorded on a spectrometer 60SX (Nicolet Instruments, Madison, WI) equipped with a Hg/Cd/Te detector and a KRS-5 polarizer (Eurolabo, Paris, France). Films of air-dried porin were tilted at  $40^\circ$  with respect to the IR beam which was linearly polarized parallel (to record  $A_{\parallel}$ ) or perpendicular (to record  $A_{\perp}$ ) to the plane of incidence, as described in 7. FTIR absorbance and linear dichroism spectra were obtained from  $(2A_{\perp} + A_{\parallel})/3$  and  $A_{\parallel} - A_{\perp}$  respectively (7). The method for the IR dichroism analysis and calculation of the average tilt angle  $\theta_M$  of the amide transition moments has been described in 7, 18. Briefly, the distribution of a set of transition

Please address all reprint requests to Dr. E. Nabedryk Service de Biophysique, Département de Biologie, CEN Saclay 91191 Gif-Sur-Yvette Cedex, France.

moments corresponding to a given absorption band can be characterized by an order parameter  $S = (3 \cos^2 \theta_M - 1)/2$ , where  $\theta_M$  is the angle between the transition moment and the normal to the disc. The dichroic ratio  $D = A_{\parallel}/A_{\perp}$  measured at a tilt angle  $i$  is related to the  $S$  by applying the relation in (7):

$$D = [3S/(1 - S)] [\sin^2 i/n^2] + 1,$$

where  $n$ , the refractive index of the layer of air-dried lipids was taken as 1.5 (7). Then, from the measured dichroic ratio, we can calculate the mean orientation of the transition vector. Second-derivative spectra were calculated with the Nicolet software parameter DR2.

## RESULTS

The FTIR absorbance spectrum of air-dried multilayers of porin (calculated from  $A_{\parallel}$  and  $A_{\perp}$  as described in reference 7) is presented in Fig. 1 *Aa*. In agreement with Kleffel et al. (4), this spectrum shows the amide I (80%  $C=O$  stretching) and amide II (60%  $N-H$  bending) bands with major components at 1,631 and 1,530  $\text{cm}^{-1}$  respectively, indicating that  $\beta$ -pleated sheets are the predominant type of protein secondary structure in porin. Several shoulders are observed  $\sim 1,650$ – $1,675 \text{ cm}^{-1}$  and at 1,696  $\text{cm}^{-1}$  on the amide I band and at 1,516  $\text{cm}^{-1}$  on the amide II band. The band at 1,737  $\text{cm}^{-1}$  is due to the absorption of the ester carbonyl groups from the lipids.

A more detailed analysis of the peaks' frequencies of the characteristic secondary structure components can be made by second-derivative analysis of the IR spectra (19, 20). The second-derivative spectrum generated from Fig. 1 *Aa* and displayed on Fig. 1 *Ba* shows three main peaks at 1,516, 1,631, and 1,697  $\text{cm}^{-1}$  as well as several very weak but reproducible bands at 1,651, 1,657, 1,672, and 1,679  $\text{cm}^{-1}$  for the amide I band and at 1,530, 1,536, and 1,563  $\text{cm}^{-1}$  for the amide II band. Tentative assignments of the main bands to specific secondary structure components and individual amino acid groups are given in Table I according to 20–22.

The IR dichroism spectrum of a film of porin is presented in Fig. 1 *Ca*. The main dichroic signals peak at 1,738 (–), 1,698 (+), 1,660 (–), 1,634 (+), and 1,531 (+)  $\text{cm}^{-1}$ . In order to remove the major source of reflection occurring at the membrane/air interface, the polarized FTIR spectra were measured with the air-dried membrane multilayers covered with Nujol, a spectroscopic grade paraffin oil commonly used in IR dichroism studies (23–26). As seen in Fig. 1, Nujol alters neither the absorption spectrum (Fig. 1 *A*) nor the position of the bands in the second-derivative spectrum (Fig. 1 *B*) nor the extent of the dichroism of the main bands (Fig. 1 *C*). This observation, together with the unperturbed dichroism of the ester  $C=O$  lipid groups at 1,738  $\text{cm}^{-1}$ , indicates that the sample has not been disordered by the Nujol treatment. However, the dichroism signal around 1,600  $\text{cm}^{-1}$  is modified. This point will be discussed later.

Qualitatively, a positive ( $A_{\parallel} - A_{\perp}$ ) dichroism signal is associated with the alignment of the oscillators at  $<55^\circ$  from the membrane normal (7, 18). The negative signal at

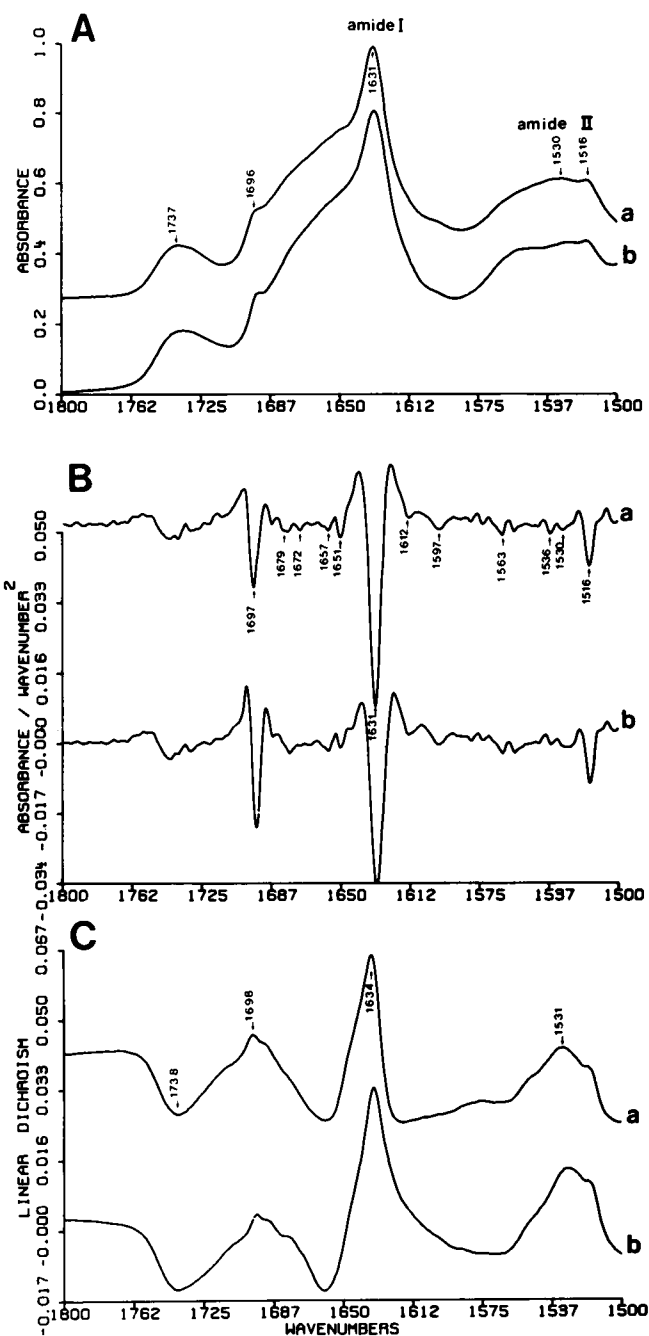


FIGURE 1 FTIR spectra of oriented films of porin reconstituted in lipid vesicles (a) without and (b) with a covering of Nujol. (A) Absorbance spectra. (B) Second-derivative spectra. The labeled peaks correspond to reproducible features observed on at least three different films. (C) Linear dichroism spectra ( $A_{\parallel} - A_{\perp}$ ). Measuring conditions: 256 scans, Resolution: 4  $\text{cm}^{-1}$ ,  $T = 20^\circ\text{C}$ .

1,738  $\text{cm}^{-1}$  thus indicates that the  $C=O$  lipid groups tend to be preferentially in the membrane plane as previously detected in native or reconstituted membranes (13–16, 18). The positive dichroism signal at 1,516  $\text{cm}^{-1}$  (Fig. 1 *C*) which corresponds to a shoulder on the amide II absorption band (Fig. 1 *A*) and to a main peak in the corresponding second-derivative spectrum (Fig. 1 *B*) can be attributed to

TABLE I  
TENTATIVE BANDS ASSIGNMENTS OF PORIN FROM  
THE SECOND-DERIVATIVE IR SPECTRA  
ACCORDING TO [20–22]

Band position	Assignment
cm <sup>-1</sup>	
1516 (VS)	Tyr
1530 (VW)	$\beta$ -sheet
1536 (W)	$\beta$ -sheet and/or $\beta$ -turns
1631 (VS)	$\beta$ -sheet
1651 (W)	unordered structure
1672 (VW)	$\beta$ -sheet and/or $\beta$ -turns
1679 (W)	$\beta$ -turns and antiparallel $\beta$ -sheets
1697 (VS)	$\beta$ -turns

S = strong, W = weak, VS = very strong, and VW = very weak.

Tyr C—C ring-stretching vibrations (27) and thus indicates that, on the average, the Tyr cycles are preferentially oriented along the normal to the membrane in porin. The positive sign of the dichroism under the main amide I (1,634 cm<sup>-1</sup>) and amide II (1,531 cm<sup>-1</sup>) components indicates that the transition moments of the amide I and amide II bands are oriented at <55° with respect to the membrane normal. Furthermore, the small magnitude of the dichroism of the amide bands suggests an average orientation of the corresponding vibration transitions at a value not too far from the magic angle ( $\theta = 55^\circ$ ). In the antiparallel  $\beta$ -pleated sheet, the C = 0 and N—H peptide bonds are mostly perpendicular to the  $\beta$ -strands direction and the strongest amide I transition component at ~1,630 cm<sup>-1</sup> is essentially polarized in the plane of the  $\beta$ -sheet along the hydrogen bond direction i.e., perpendicular to the chain axis while the amide II transition is polarized along the chain axis (28, 29). Qualitatively, from our IR dichroism data (Fig. 1 C), it thus appears that a  $\beta$ -sheet arrangement with all strands strictly perpendicular or parallel to the membrane can be excluded.

It has been previously reported that distortions of the amide I and amide II bands brought about by optical reflection effects can be observed in the IR dichroism spectra of proteins (25, 26). We found that these effects are mostly evident in samples with small amounts of dichroism (e.g., air-dried films of soluble proteins such as cytochrome c or ribonuclease A; [Tiede D., E. Nabedryk, and J. Breton, unpublished data]). These effects appear to be present to about the same extent but are largely hidden in samples with large dichroic signals (e.g., purple membrane for which almost no change is observed upon Nujol addition; [Nabedryk E., and J. Breton, unpublished results]). We have previously reported the use of Nujol to decrease the optical interference and dispersion effects in IR linear dichroism spectra of films of photosynthetic membranes and of several reaction centers and antenna complexes reconstituted in lipid vesicles (15, 16, 25). In particular, the IR dichroism spectrum of air-dried oriented

reaction centers without Nujol (13) shows in addition to the large positive signal at 1,656 cm<sup>-1</sup> (indicative of transmembrane  $\alpha$ -helices) a small negative signal ~1,630 cm<sup>-1</sup>. Upon addition of Nujol (16, 25), this negative signal is removed and the amide I dichroism signal is now more symmetrical. These modifications have been attributed to a decrease of the optical interference and dispersion effects arising from multiple reflections occurring at the various dielectric interfaces present in an air-dried sample (23–26). In these experiments, it should be noted that both the extent of the  $\alpha$ -helix orientation and the visible linear dichroism of the chromophores are essentially unperturbed when the film of reaction centers is covered with Nujol indicating the absence of significant structural changes.

In the case of porin, the dichroism signal on the lower wave number side (at ~1,600 cm<sup>-1</sup>) of the amide I band is also modified upon addition of Nujol (Fig. 1 Cb). However, the tilt angle values calculated from both types of spectra (Fig. 1 Ca and b) are similar indicating an identical orientation of  $\beta$ -sheets. For a quantitative determination of the average  $\beta$ -strands orientation in porin, the amide I and amide II bands are treated independently. For the amide I, assuming that the dichroism at 1,634 cm<sup>-1</sup> is only due to the orientation of the  $\beta$ -sheet secondary structure, the experimental dichroic ratio  $D = A_{\parallel}/A_{\perp}$  is used to calculate the angle  $\theta_{MI}$  of the amide I transition moment with respect to the normal to the membrane plane. For the amide II band, a correction is applied to the experimental dichroic ratio to account for some overlap of the different types of secondary structures within the amide II signal. Using a 68%  $\beta$ -sheet content, estimated by analyzing UV circular dichroism spectra of porin by a linear square curve-fitting procedure (data not shown), and assuming an equal extinction coefficient for  $\beta$ -sheet and random conformation, the corrected dichroic ratio  $D_c$  for only  $\beta$ -sheets is calculated and then the tilt angle  $\theta_{MII}$ . These  $D$ ,  $D_c$ , and  $\theta_M$  values are summarized in Table II. The dichroic ratios of the amide I and amide II bands lead to almost identical  $\theta_{MI}$  and  $\theta_{MII}$  values i.e.,  $47^\circ \pm 3^\circ$ .

## DISCUSSION

The evidence in favor of a large amount of  $\beta$ -pleated sheets in the porin with no detectable  $\alpha$ -helix is supported by a variety of spectroscopic and diffraction measurements (3–5, 30) as well as prediction from amino acid sequence analysis (30, 31). In particular, x-ray diffraction studies on

TABLE II  
ESTIMATION OF  $D$ ,  $D_c$ , AND  $\theta_M$  OF PORIN FROM  
INFRARED DICHROISM DATA

Amide I		Amide II	
$D$	$\theta_{MI}$	$D_c$	$\theta_{MII}$
1.10	48°	1.13	47°

The average was obtained from three different air-dried samples.

3-D crystals (4) demonstrated that a significant fraction of the  $\beta$ -strands are oriented at a very small angle to the membrane normal as indicated by the existence and widths of the 3.5 and 4.6 Å meridional reflections. The equatorial diffraction maxima also support the existence of antiparallel  $\beta$ -structure. Porin thus differs from the larger class of transmembrane proteins such as bacteriorhodopsin from *Halobacterium halobium* or reaction center from purple photosynthetic bacteria in which several  $\alpha$ -helical segments span the membrane with a small tilt with respect to the normal to the membrane plane (6–8, 13, 16). It also differs in its very polar character (31). Since porin functions as a membrane pore, the question then arises of how membrane-spanning  $\beta$ -sheets containing polar residues could be accommodated within a hydrophobic membrane domain in such a way that pores are formed. The cylindrical arrangement of  $\beta$ -sheets within the membrane into the so-called “ $\beta$ -sheet barrel” has been discussed as a possible model of the intramembranous regions of integral membrane proteins (32). In the  $\beta$ -sheet barrel described by Kennedy (32), the  $\beta$ -strands run roughly parallel to the axis of the cylinder. Such a model would be expected to fit into a membrane provided the outside of the protein would be predominantly hydrophobic. Indeed, such a folding pattern for the porin has recently been proposed from Raman studies and structural predictions (30).

The present IR data confirms the existence of antiparallel  $\beta$ -sheet structure as the dominant secondary structure of porin. Furthermore, from our IR dichroism spectra, it can be calculated that the average orientation ( $\theta_M$ ) of the amide I and amide II transition moments of the  $\beta$ -sheet is at  $47^\circ \pm 3^\circ$  from the membrane normal. As the main components of the amide I and amide II transition moments are polarized along the hydrogen-bond direction and along the chain axis, respectively (28, 29), it thus appears that the average angle  $\bar{\theta}$  of inclination away from the membrane normal for the  $\beta$ -strands is  $\sim 45^\circ$ . This applies severe constraints on the  $\beta$ -sheet orientations that could exist in porin, particularly when the diffuse x-ray data of Kleffel et al. (4) reveal that a substantial number of the  $\beta$ -strands are nearly perpendicular to the membrane plane. A  $\beta$ -barrel arrangement as proposed by Kennedy (32) would not be consistent with the experimental observations although our IR data would be compatible with a cylindrical  $\beta$ -structure recently described by Pryciak et al. (33) in which the  $\beta$ -strands are tilted at  $\sim 45^\circ$  from the cylinder axis. Having all the  $\beta$ -strands inclined away from the membrane normal (Fig. 2, *a* and *b*) which fits the IR results, would however be inconsistent with the x-ray data. One arrangement of  $\beta$ -strands (Fig. 2 *c*) does satisfy both requirements that a significant fraction of the  $\beta$ -strands are nearly aligned along the membrane normal (4), yet the average strand orientation away from the membrane normal is  $\sim 45^\circ$ . In this model (Fig. 2 *c*), each porin monomer consists of two domains of  $\beta$ -sheet both with their plane perpendicular to the membrane plane, one having its

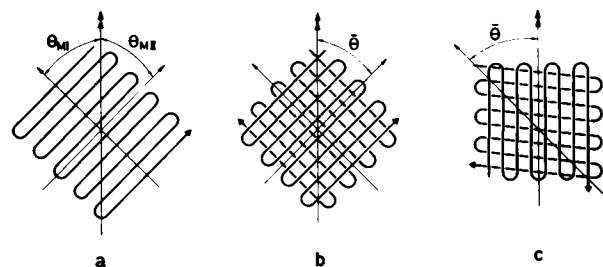


FIGURE 2 Possible models for the packing of  $\beta$ -strands in porin monomer. The double arrowheads represent the direction of the membrane normal  $N$ . The single arrowhead in *a* represents the direction of the amide I ( $\theta_{MI}$ ) and amide II ( $\theta_{MII}$ ) transition moments;  $\bar{\theta}$  is the average tilt angle of the  $\beta$ -strands. In *a* and *b* all the strands are inclined at some average angle away from the membrane normal. This kind of strand arrangement would not give rise to the x-ray results of Kleffel et al. (4) though it is consistent with the IR results. However, a  $\beta$ -sheet sandwich shown in *c* could give rise to the  $\theta_M$  value of  $47^\circ \pm 3^\circ$  found in the IR experiments depending on the number and orientation of  $\beta$ -strands in each sheet. Furthermore, having one sheet with its strand directions parallel to the membrane normal could account for the diffuse diffraction observation of Kleffel et al. (4).

strands direction lying nearly parallel to the membrane normal, and the other having its strands inclined close to the membrane plane. The angle between the strands of the two sheets is large and could approach  $90^\circ$ . The positions of these sheets within the porin monomer are not known. However, close contact of the sheets could create an orthogonally packed  $\beta$ -sheet super-structure similar to those seen in soluble proteins (34).

Predictions of secondary structure (30, 31) suggest that up to 16–18  $\beta$ -strands ( $11 \pm 5$  residues long) make up most of the porin structure. This number of strands would be sufficient to form two large sheets. Vogel and Jähnig (30) also suggest that up to 12  $\beta$ -strands are amphipathic as detected by hydrophobicity correlation. Since amphipathic  $\beta$ -strands can generate a discrete hydrophobic surface, we propose that these strands form the  $\beta$ -sheet domain which is in direct contact with the lipids. The  $\beta$ -strand directions of this outer sheet would be perpendicular to the membrane plane (Fig. 2 *c*) and thus allow the polypeptide chain to follow the shortest traverse through the membrane and to use the minimal amount of amino acid residues to form the outside surface of the protein. A continuous  $\beta$ -sheet structure at the protein-lipid interface would now be created as the porin trimer assembles in the membrane. Within each monomer the second  $\beta$ -sheet, with its strand directions inclined quite close to (or even along) the membrane plane (Fig. 2 *c*) and its plane also perpendicular to the membrane, would be involved in the protein-protein interactions responsible for the subunit contacts and perhaps the pore structure.

The question of how the pores are constructed is still open. The kind of  $\beta$ -sheet arrangement we are proposing makes it difficult to envisage a pore built within single monomers, created only by  $\beta$ -sheet interactions. It must be remembered, however, that about one-third of the polypep-

tide is not involved in  $\beta$ -sheet structures. Furthermore, the pores can be located at the subunit interfaces of the trimer where the structural elements forming the pores need not be  $\beta$ -sheet. Our IR results and the earlier x-ray results (4) only allow us to deduce that the porin monomer is composed of at least two  $\beta$ -sheet structural domains, which are oriented nearly orthogonal with respect to each other. We have no information if they are formed from continuous segments of the amino acid sequence (as crudely depicted in Fig. 2c). Furthermore, it must be emphasized that the model of the  $\beta$ -sheet arrangement derived from our IR dichroism data cannot be quantitative. We have assumed that the amide I and amide II transition moments are ideally at  $90^\circ$  and  $0^\circ$ , respectively, from the  $\beta$ -strand axis. Distortions and twists of the  $\beta$ -strands can lead to deviations in these angular values. Hence while a sandwiched  $\beta$ -sheet arrangement is consistent with the experimental observations, the precise angle of inclination of the sheets cannot be estimated without additional structural information. Nevertheless, the experimental data show that the porin structure is more convoluted than previously expected. A 3-D structure of this pore protein (see reference 5) would add a great deal of information concerning the variety of polypeptide configurations that can exist in biological membranes.

We would like to thank Dr. J.P. Rosenbusch and his group for their help in purifying *E. coli* porin for our structural experiments. We acknowledge the help of Dr. W. Welte in the early stage of the project. We also thank A.-M. Bardin for UV circular dichroism measurements.

This work was partially supported by the Swiss National Foundation grant 3.622.84 to R. M. Garavito.

Received for publication 24 June 1987 and in final form 9 December 1987.

## REFERENCES

- Engel, A., A. Massalski, H. Schindler, D. L. Dorset, and J. P. Rosenbusch. 1985. Porin channel triplets merge into single outlets in *Escherichia coli* outer membranes. *Nature (Lond.)* 317:643-645.
- Dorset, D. L., A. Engel, M. Häner, A. Massalski, and J. P. Rosenbusch. 1983. Two-dimensional crystal packing of matrix porin. A channel forming protein in *Escherichia coli* outer membranes. *J. Mol. Biol.* 165:701-710.
- Rosenbusch, J. P. 1974. Characterization of the major envelope protein from *Escherichia coli*. Regular arrangement on the peptidoglycan and unusual dodecyl sulfate binding. *J. Biol. Chem.* 249:8019-8029.
- Kleffel, B., R. M. Garavito, W. Baumeister, and J. P. Rosenbusch. 1985. Secondary structure of a channel-forming protein: porin from *E. coli* outer membranes. *EMBO (Eur. Mol. Biol. Organ.) J.* 4:1589-1592.
- Garavito, R. M., J. Jenkins, J. N. Jansonius, R. Karlsson, and J. P. Rosenbusch. 1983. X-ray diffraction analysis of matrix porin, an integral membrane from *Escherichia coli* outer membranes. *J. Mol. Biol.* 164:313-327.
- Rothschild, K. J., and N. A. Clark. 1979. Polarized infrared spectroscopy of oriented purple membrane. *Biophys. J.* 25:473-488.
- Nabedryk, E., and J. Breton. 1981. Orientation of intrinsic proteins in photosynthetic membranes. Polarized infrared spectroscopy of chloroplasts and chromatophores. *Biochim. Biophys. Acta.* 635:515-524.
- Nabedryk, E., A.-M. Bardin, and J. Breton. 1985. Further characterization of protein secondary structures in purple membrane by circular dichroism and polarized infrared spectroscopies. *Biophys. J.* 48:873-876.
- Nabedryk, E., and J. Breton. 1986. Polarized Fourier transform infrared (FTIR) difference spectroscopy of the  $M_{412}$  intermediate in the bacteriorhodopsin photocycle. *FEBS (Fed. Eur. Biochem. Soc.) Lett.* 202:356-360.
- Michel-Villaz, M., H. R. Saibil, and M. Chabre. 1979. Orientation of rhodopsin  $\alpha$ -helices in retinal rod outer segment membranes studied by infrared linear dichroism. *Proc. Natl. Acad. Sci. USA.* 76:4405-4408.
- Rothschild, K. J., R. Sanches, T. L. Hsiao, and N. A. Clark. 1980. A spectroscopic study of rhodopsin  $\alpha$ -helix orientation. *Biophys. J.* 31:53-64.
- Bazzi, M. D., and R. W. Woody. 1985. Oriented secondary structure in integral membrane proteins. I. Circular dichroism and infrared spectroscopy of cytochrome oxidase in multilamellar films. *Bio-phys. J.* 48:957-966.
- Nabedryk, E., D. M. Tiede, P. L. Dutton, and J. Breton. 1982. Conformation and orientation of the protein in the bacterial photosynthetic reaction center. *Biochim. Biophys. Acta.* 682:273-280.
- Breton, J., and E. Nabedryk. 1984. Transmembrane orientation of  $\alpha$ -helices and the organization of chlorophylls in photosynthetic pigment-protein complexes. *FEBS (Fed. Eur. Biochem. Soc.) Lett.* 176:355-359.
- Nabedryk, E., S. Andrianambinintsoa, and J. Breton. 1984. Transmembrane orientation of  $\alpha$ -helices in the thylakoid membrane and in the light-harvesting complex. A polarized infrared spectroscopy study. *Biochim. Biophys. Acta.* 765:380-387.
- Nabedryk, E., G. Berger, S. Andrianambinintsoa, and J. Breton. 1985. Comparison of  $\alpha$ -helix orientation in the chromatophore, quantasome, and reaction centre of *Rhodospseudomonas viridis* by circular dichroism and polarized infrared spectroscopy. *Biochim. Biophys. Acta.* 809:271-276.
- Schindler, H., and J. P. Rosenbusch. 1981. Matrix protein in planar membranes: clusters of channels in a native environment and their functional reassembly. *Proc. Natl. Acad. Sci. USA.* 78:2302-2306.
- Nabedryk, E., M. P. Gingold, and J. Breton. 1982. Orientation of gramicidin A transmembrane channel. Infrared dichroism study of gramicidin in vesicles. *Biophys. J.* 38:243-249.
- Susi, H., and D. M. Byler. 1983. Protein structure by Fourier transform infrared spectroscopy: second derivative spectra. *Bio-chem. Biophys. Res. Commun.* 115:391-397.
- Byler, D. M., and H. Susi. 1986. Examination of the secondary structure of proteins by deconvolved FTIR spectra. *Biopolymers.* 25:469-487.
- Miyazawa, T., and E. R. Blout. 1961. The Infrared Spectra of Polypeptides in Various Conformations: Amide I and II Bands. *J. Am. Chem. Soc.* 83:712-719.
- Bandekar, J., and S. Krimm. 1979. Vibrational analysis of peptides, polypeptides, and proteins: Characteristic amide bands of  $\beta$ -turns. *Proc. Natl. Acad. Sci. USA.* 76:774-777.
- Lutinski, C. 1958. Method for elimination of interference fringes in spectra of thin films. *Anal. Chem.* 30:2071-2072.
- Jasse, B., and J. L. Koenig. 1979. Orientational measurements in polymers using vibrational spectroscopy. *J. Macromol. Sci. Rev. Macromol. Chem.* 17:6-35.
- Nabedryk, E., D. Tiede, P. L. Dutton, and J. Breton. 1984. Polarized infrared spectroscopy of bacterial reaction centers: the LMH and LM complexes in reconstituted membrane. In *Advances in Photosynthesis Research* C. Sybesma, editor. Vol. II. 177-180. Martinus Nijhoff/Dr. W. Junk Publishers, Dordrecht, The Netherlands.

26. Tiede, D. M. 1985. Incorporation of membrane proteins into interfacial films: model membranes for electrical and structural characterization. *Biochim. Biophys. Acta.* 811:357-379.
27. Bendit, E. B. 1967. Infrared absorption of tyrosine side chains in proteins. *Biopolymers.* 5:525-533.
28. Miyazawa, T. 1960. Perturbation treatment of the characteristic vibrations of polypeptide chains in various configurations. *J. Am. Chem. Soc.* 32:1647-1652.
29. Suzuki, E. 1967. A quantitative study of the amide vibrations in the infra-red spectrum of silk fibroin. *Spectrochimica Acta Part A Mol. Spectrosc.* 23A:2303-2308.
30. Vogel, H., and F. Jähnig. 1986. Models for the structure of outer-membrane proteins of *Escherichia coli* derived from Raman spectroscopy and prediction methods. *J. Mol. Biol.* 190:191-199.
31. Paul, C., and J. P. Rosenbusch. 1985. Folding patterns of porin and bacteriorhodopsin. *EMBO (Eur. Mol. Biol. Organ.) J.* 4:1593-1597.
32. Kennedy, S. J. 1978. Structures of membrane proteins. *J. Membr. Biol.* 42:265-279.
33. Pryciak, P. M., J. D. Conway, F. A. Eiserling, and D. Eisenberg. 1986. Cylindrical beta structure: a hypothetical protein structure. *In Protein Structure, Folding, and Design.* (D. L. Oxender, editor.) 39:243-246. Alan R. Liss, Inc., NY.
34. Chothia, C., and J. Janin. 1982. Orthogonal packing of  $\beta$ -pleated sheets in proteins. *Biochemistry.* 21:3955-3965.